International Journal of Marine Engineering Innovation and Research, Vol. 11(1), Mar. 2026. 67-76
(pISSN: 2541-5972, eISSN: 2548-1479)

Structural Integrity and Edge Stiffness Evaluation of GFRP Modular Towing Tank: Analytical and Numerical Study

M. Muslim, A. Buwono, Moch. Ricky Dariansyah, M. Danil Arifin, Aldyn Clinton P.O,
S. Permana[2*], M. A'Zom Ar-Rabaqi[2*]

(Received: 27 February 2026 / Revised: 1 March 2026 / Accepted: 5 March 2026 / Available Online: 13 March 2026)

***Abstract*—** Conventional hydrodynamic testing facilities require substantial capital investment, limiting maritime research accessibility in developing nations. This study addresses the structural integrity and global stiffness challenges in designing a modular Glass Fiber Reinforced Polymer (GFRP) composite towing tank as a cost-effective alternative. A hybrid laminate configuration combining Chopped Strand Mat 450 g/m² and Woven Roving 800 g/m² was analyzed under hydrostatic loading using Classical Laminate Theory (CLT) and Finite Element Method (FEM). Analytical predictions indicated acceptable performance with 26.09 MPa bending stress and 5.95 mm deflection under fully clamped boundary assumptions. However, full-scale FEM simulation revealed critical free-edge effects, producing 41 MPa Von Mises stress and 62 mm deflection at the tank rim exceeding the L/200 serviceability limit despite maintaining a safety factor of 3.65. This study demonstrates that while the 19 mm wall thickness satisfies strength requirements per ASME RTP-1 standards, edge stiffening through horizontal rim reinforcement is essential to control excessive deformation in open-top modular configurations.

Keywords— Towing Tank, Composite Materials, GFRP, Structural Analysis, Finite Element Method.

**Corresponding Author: sulaksana@yahoo.com, muhammadazom650@gmail.com*

I. INTRODUCTION

The global maritime industry is currently undergoing a massive transformation driven by the imperative to decarbonize shipping operations. The ambitious targets established by the International Maritime Organization (IMO) to achieve a 50% reduction in greenhouse gas emissions by 2050 necessitate radical innovations in energy-efficient hull forms and advanced propulsion systems[1]. For archipelagic nations such as Indonesia, developing these technologies is not merely a matter of environmental compliance but a strategic pillar in realizing the vision of the Global Maritime Fulcrum as mandated in the National Research Master Plan (RIRN) 2017-2045[2]. Consequently, the demand for precise hydrodynamic testing infrastructure has surged dramatically. Although computational fluid dynamics (CFD) has advanced significantly in recent years, empirical validation through physical towing tank testing remains the irreplaceable gold standard for verifying ship resistance predictions and propulsion efficiency[3]. However, establishing conventional reinforced concrete hydrodynamic testing facilities demands capital expenditures exceeding USD 5-10 million and extensive permanent land allocation. This creates a prohibitive entry barrier for vocational education institutions and medium-scale shipyards in developing economies, ultimately hindering the acceleration of national maritime innovation and technological independence[4]. Thus, developing a low-cost, modular, and scalable testing facility has become critically important for democratizing access to maritime research infrastructure.

To overcome these financial and spatial constraints, Glass Fiber Reinforced Polymer (GFRP) composite materials offer a highly viable structural solution. GFRP provides an exceptional strength-to-weight ratio, superior corrosion resistance in aquatic environments, ease of fabrication through hand lay-up or resin infusion processes, and inherent modularity that enables facility relocation and dimensional scalability[5]. In recent years, the state of the art in composite engineering has extensively explored GFRP's mechanical behavior and structural applications in marine environments. Various studies have confirmed its long-term reliability against osmotic degradation, ultraviolet exposure, and seawater-induced hydrolysis in harsh offshore conditions[6][7]. Mai et al. [5] demonstrated that GFRP bars maintain 85% of their initial tensile strength after three years of seawater immersion, validating the material's suitability for permanent water-contact applications. Furthermore, numerous researchers have successfully optimized composite laminate designs for fluid-containment structures, predominantly focusing on cylindrical pressure vessels, spherical tanks, or fully enclosed rectangular containers[8][9]. These pioneering studies have established robust analytical and numerical methodologies for predicting material failure under uniform internal pressure using classical laminate theory and various finite element analysis techniques[10][11].

Muswar Muslim, Darma Persada University, Indonesia, E-mail: muslim.muswar@gmail.com
Ayom Buwono, Darma Persada University, Indonesia, Email: abuwono.energi@gmail.com
Moch. Ricky Dariansyah, Darma Persada University, Indonesia, Email: ricky.nautical@yahoo.com
Mohammad Danil Arifin, Darma Persada University, Indonesia, Email: danilarifinmohammad@gmail.com
Aldyn Clinton Partahi Oloan, Darma Persada University, Indonesia, Email: clintonaldyn19@gmail.com
Sulaksana Permana, Gunadarma University, Indonesia, Email: sulaksana@yahoo.com
Muhammad A'Zom Ar-Rabaqi, Gunadarma University, Indonesia, Email: muhammadazom650@gmail.com

Rashid et al. [7] specifically investigated hybrid configurations combining Woven Roving (WR) and Chopped Strand Mat (CSM) fibers, concluding that alternating layup sequences achieve balanced in-plane orthotropic properties crucial for rectangular geometries subjected to biaxial loading.

Despite these significant advancements, a critical gap persists in the structural design and analysis of long, rectangular, open-top composite tanks intended for precision hydrodynamic testing applications. Current engineering practices often mistakenly apply cylindrical hoop stress formulations derived from Barlow's equation to rectangular tanks, completely ignoring the fundamental physical reality that flat-walled tanks are dominated by transverse plate bending moments rather than membrane tension stresses[12]. This conceptual error leads to grossly unconservative deflection predictions. Moreover, while some researchers have utilized classical Kirchhoff-Love plate theories to design rectangular composite containers, they frequently isolate a single panel segment and assume perfectly clamped boundary conditions on all four edges [13][14]. This reductionist approach entirely neglects the global structural behavior of full-scale assemblies where inter-module joint flexibility and edge restraint conditions dramatically influence overall stiffness. Specifically, for an open-top towing tank configuration where the upper rim remains free to facilitate model carriage operations and water filling procedures, the loss of lateral restraint at this critical edge becomes a governing design concern that can trigger excessive outward bulging and geometric instability phenomena that idealized partial analytical models fundamentally fail to predict[15]. Li et al. [16] analytically demonstrated that rectangular plates with free edges experience deflection amplification factors ranging from 8× to 12× compared to fully clamped counterparts, yet this finding has rarely been incorporated into practical composite tank design procedures. Furthermore, existing literature predominantly addresses ultimate strength verification through failure criteria such as Tsai-Wu or Tsai-Hill, while systematically neglecting serviceability limit states particularly critical for precision measurement facilities where excessive wall deflection directly compromises the geometric accuracy of towing carriage rails and introduces systematic errors in resistance measurements[17].

Therefore, the novelty of this research lies in comprehensively identifying and quantitatively evaluating the often-ignored global edge stiffness effects and critical deformation modes of a full-scale, open-top modular composite towing tank through rigorous comparative analysis. By systematically juxtaposing classical idealized analytical plate theories assuming rigid boundary conditions with a comprehensive full-scale three-dimensional numerical simulation incorporating realistic open-top geometry and bolted flange joints, this paper exposes the inherent dangers and quantifies the magnitude of error introduced by relying on simplified boundary assumptions in maritime composite infrastructure design. Unlike prior investigations that focus on isolated panel behavior, this study uniquely demonstrates that for open-top fluid-containment infrastructures operating under hydrostatic loading, global structural stiffness rather than localized material strength emerges as the definitive governing design parameter. The research further establishes that conventional safety factor approaches based solely on ultimate tensile strength criteria are insufficient; designers must simultaneously satisfy deflection-based serviceability requirements to ensure operational functionality. This dual validation framework represents a paradigm shift from strength-driven design to stiffness-driven design philosophy, particularly relevant for precision engineering applications where geometric tolerances are paramount.

The primary objective of this study is to rigorously evaluate the structural integrity and systematically optimize the global stiffness characteristics of a 10-meter modular GFRP towing tank subjected to non-uniform hydrostatic loading up to a 2-meter water depth. The specific aims encompass four key technical contributions. First, to correct the conventional oversimplified design approach by properly applying Kirchhoff-Love plate theory with equivalent uniform load transformations to establish baseline analytical predictions under idealized boundary conditions. Second, to validate the actual structural response through a full-scale Finite Element Method (FEM) simulation explicitly incorporating realistic free-edge boundary conditions at the tank rim, second-order shell elements for accurate bending behavior capture, and the Tsai-Hill orthotropic failure criterion appropriate for laminated composites. Third, to quantify the disparity magnitude between analytical predictions and numerical reality, thereby establishing correction factors for future design codes governing modular composite hydrodynamic facilities. Fourth, to formulate concrete, actionable engineering design recommendations including optimal rim stiffener specifications that ensure the facility successfully satisfies both ultimate limit state requirements per ASME RTP-1 standards and serviceability limit state deflection tolerances per precision measurement facility guidelines. Through these contributions, this research provides a validated design methodology that enables developing nations to deploy cost-effective maritime research infrastructure, directly supporting technological independence and innovation acceleration in the naval architecture sector.

II. METHOD

II.1 *Research Method*

This research adopts a rigorous comparative-quantitative approach that systematically integrates analytical calculations based on Classical Laminate Theory (CLT) with comprehensive numerical simulations employing the Finite Element Method (FEM). The overarching research strategy is deliberately designed to validate the structural integrity and global stiffness characteristics of the tank wall design prior to committing resources to physical fabrication, thereby proactively mitigating potential material failure risks and minimizing cost inefficiencies associated with iterative prototype testing[14].

The investigation workflow commences with an extensive literature review to establish the theoretical foundation and identify design parameters validated in prior composite tank research. Subsequently, critical material properties are defined through a combination of manufacturer datasheets, industry standards (BKI Volume V, ASTM test protocols), and the Rule of Mixtures for hybrid fiber composites[18]. The laminate architecture is then systematically configured, specifying the stacking sequence, fiber orientations, and consolidated thickness required to withstand the design hydrostatic loading.

Following material and geometry definition, analytical predictions are generated using Roark's plate formulas adapted for rectangular panels under non-uniform pressure distributions. These closed-form solutions provide baseline stress and deflection estimates assuming idealized boundary conditions. Concurrently, a high-fidelity three-dimensional finite element model is constructed incorporating realistic geometric features, material orthotropy, and operational boundary constraints. The analytical and numerical results are then collected and subjected to rigorous quantitative comparison to identify discrepancies and understand their physical origins. A critical decision milestone occurs at the safety factor validation stage: if the computed safety factor falls below the ASME RTP-1 threshold of 3.0 for non-metallic pressure vessels, the workflow systematically reverts to the material property and laminate structure definition phase for parametric revision, potentially adjusting fiber content, layer count, or resin type[19].

Conversely, if both ultimate limit state (strength) and serviceability limit state (deflection) criteria are simultaneously satisfied, the design is deemed validated and approved for fabrication, culminating in research conclusions and actionable design recommendations. The complete research methodology flowchart, illustrating these sequential stages and decision logic, is presented in Figure 1.

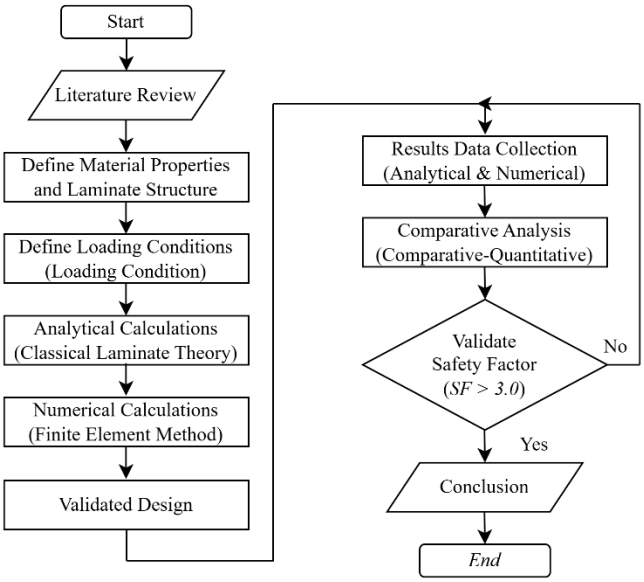

Figure 1. Flowchart of Towing Tank Research Methodology

II.2 *Geometric Configuration and Modular Concept*

The towing tank structure investigated in this study measures 10,000 mm in length, 2,000 mm in width, and 2,000 mm in height, yielding a total water containment volume of 40 cubic meters when filled to maximum operational depth. To enable practical construction, transportation, and potential relocation, the structure is segmented into five identical modules, each spanning 2,000 mm in length and interconnected through precision-machined bolted flange joints fabricated from marine-grade stainless steel (AISI 316).

This modular design philosophy confers several critical advantages for resource-constrained institutions: dimensional scalability allows the facility to be extended to 15 or 20 meters by adding standardized modules without redesigning the entire system; facility mobility permits disassembly and relocation if institutional space allocation changes; and phased construction enables initial operation with three modules while additional segments are fabricated, thereby distributing capital expenditure over multiple fiscal periods[15]. Figure 2(a) illustrates the complete 10-meter assembly in its operational configuration, while Figure 2(b) provides detailed geometry of an individual module highlighting the flanged connection interface designed to transmit shear forces and bending moments between adjacent segments. From a structural mechanics perspective, the bolted flange joints introduce a quasi-fixed boundary condition along the vertical module interfaces.

These connections provide substantial lateral restraint through friction at the bolt-tightened interfaces and mechanical interlock via precisely aligned bolt holes, effectively simulating a clamped edge condition in the vertical direction. Similarly, the tank base rests on a reinforced concrete foundation slab, which constrains translational and rotational degrees of freedom at the bottom edge, replicating a fixed support condition. However, the uppermost rim of the tank necessarily remains unrestrained to facilitate three essential operational requirements: the passage of the model towing carriage and its support rails along the tank length; unrestricted water filling and drainage access;

and accommodation of instrumentation cables connecting onboard sensors to the data acquisition system. This open-top configuration creates a free edge boundary condition at z = 2,000 mm, where no external restraint exists to oppose lateral deflection induced by hydrostatic pressure. This free-edge condition represents the most critical structural vulnerability in the design and constitutes the primary focus of this investigation.

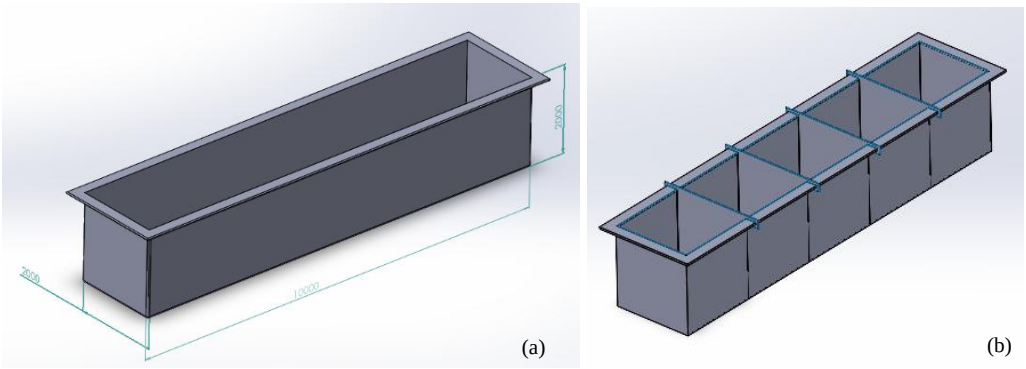

Figure 2: (a) Full 10-Meter Modular Towing Tank Assembly and (b) Individual 2-Meter Module with Flange Connection Details

II.3 *Composite Material Characterization*

The composite material system selected for this application consists of a hybrid laminate architecture combining two distinct glass fiber reinforcement types embedded in a thermoset polymer matrix. The matrix resin is Isophthalic Unsaturated Polyester (UP), specifically selected for its superior hydrolysis resistance compared to orthophthalic polyester variants commonly used in general-purpose fiberglass applications[17]. Isophthalic resins demonstrate significantly reduced water absorption rates (typically 0.15% vs. 0.30% for orthophthalic types after 24-hour immersion per ASTM D570), thereby minimizing osmotic blistering risks during prolonged water contact a failure mode that has plagued early composite marine structures. The reinforcement consists of two complementary fiber forms.

The primary load-bearing constituent is E-glass Woven Roving (WR) with an areal density of 800 g/m², featuring a balanced plain weave architecture where warp and weft yarns intersect at 90-degree angles with equal linear densities[20]. This bidirectional configuration provides orthotropic mechanical properties with equivalent tensile strengths along the 0° and 90° fiber directions, ideally suited for rectangular tank geometries subjected to biaxial hydrostatic loading. The secondary reinforcement is E-glass Chopped Strand Mat (CSM) with an areal density of 450 g/m², consisting of randomly oriented discontinuous fibers bonded with a styrene-soluble polyester binder[21].

While CSM exhibits lower absolute strength than continuous fiber fabrics, it contributes three critical functions: it provides quasi-isotropic in-plane properties that mitigate directional weaknesses; it enhances interlaminar shear strength by creating mechanical interlocking between adjacent WR plies; and it facilitates resin-rich surface layers that protect continuous fibers from direct environmental exposure. The laminate stacking sequence follows an alternating pattern formulated as [Resin-rich layer | CSM 450 | WR 800]$_{13}$, repeated thirteen times to construct a symmetric layup.

Each repeat unit contributes approximately 2.2 mm to the consolidated thickness, calculated as 0.8 mm resin-rich surface layer plus 0.6 mm for the impregnated CSM ply plus 0.8 mm for the impregnated WR ply, based on assumed fiber volume fractions of 35% for CSM and 55% for WR. The complete 26-layer laminate achieves a nominal cured thickness of 19 mm, though manufacturing variations typically introduce ±1 mm tolerance depending on hand layup compaction pressure and resin viscosity during wet-out. This hybrid architecture strategically exploits the complementary characteristics of WR and CSM: the woven fabric provides primary bending stiffness and tensile capacity along principal loading directions, while the chopped mat distributes stresses more uniformly and arrests potential delamination cracks that might propagate along continuous fiber-resin interfaces[22]. The hybrid laminate arrangement is illustrated in Figure 3.

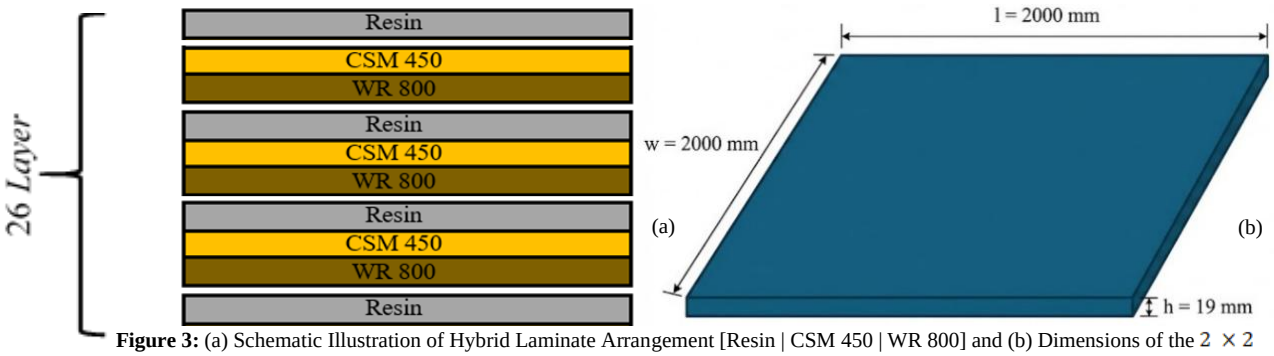

Figure 3: (a) Schematic Illustration of Hybrid Laminate Arrangement [Resin | CSM 450 | WR 800] and (b) Dimensions of the 2 × 2 Meter Towing Tank Wall

To predict the mechanical performance of this heterogeneous composite system, effective homogenized material properties must be derived from the constituent fiber and resin properties using micromechanics-based mixing rules. The classical Rule of Mixtures, validated extensively for aligned fiber composites, provides first-order estimates for longitudinal elastic modulus and tensile strength[23]. Based on the Rule of Mixtures and BKI Vol. V standards, the effective mechanical properties of the material are presented in Table 1.

TABLE 1.
MECHANICAL PROPERTIES OF HYBRID COMPOSITE MATERIAL (WR 800 + CSM 450)

Property	Symbol	Value	Reference
Density	ρ_m	$1.65\ g/cm^3$	[22][23][24]
Longitudinal Elastic Modulus	E_1	$12.5 - 15.0\ GPa$	[18][25]
Transverse Elastic Modulus	E_2	$10.0 - 12.0\ GPa$	[26][27]
Shear Modulus	G_{12}	$3.5\ GPa$	[27][23]
Poisson Ratio	ν_{12}	0.28	[28]
Ultimate Tensile Strength	X_t	$150 - 220\ MPa$	[29][30]
Ultimate Compressive Strength	X_c	$180 - 200\ MPa$	[29][30]

Note: Properties validated against ASTM D3039 (tensile), D790 (flexural), and D2344 (shear) test standards.

II.4 *Hydrostatic Pressure Distribution*

In contrast to the cylindrical pressure vessel approach ($\sigma = Pr/t$), which is often misapplied to rectangular tanks, this study applies the Kirchhoff-Love Plate Theory for thin plates undergoing pure bending[31][32]. The hydrostatic load distribution (q) is defined as a linear function of depth (z):

$$P(z) = \rho_w \cdot g \cdot z \quad \text{..... (1)}$$

Where;
$\rho_w = 1{,}000\ \mathrm{kg/m^3}$ mass density of freshwater at 20°C,
$g = 9.81\mathrm{m/s^2}$ is the standard gravitational acceleration,
z = depth from water surface (m)

At the tank base (z = 2.0 m), the maximum pressure reaches $P_{max} = 1{,}000(9.81)(2.0) = 19{,}620$ Pa.

II.5 *Analytical Calculation*

Referring to Roark's Formulas for Stress and Strain (case 2: rectangular plate, all edges fixed)[33][34], the maximum bending stress (σ_{max}) and maximum deflection (y_{max}) are calculated using the following equations. For thin rectangular plates undergoing transverse loading with small deflections ($w/t < 1/5$), Kirchhoff-Love assumptions are valid. Roark's Formulas provide closed-form solutions for bending stress and deflection:

$$\sigma_{max} = \beta \cdot \frac{P_{max} \cdot b^2}{t^2} \quad \text{..... (2)}$$

$$y_{max} = \alpha \cdot \frac{P_{max} \cdot b^4}{E \cdot t^3} \quad \text{..... (3)}$$

Where:
q = uniform equivalent load (Pa)
b = short dimension of panel (2,000 mm)
t = wall thickness (19 mm)
α, β = dimensionless coefficients based on the panel aspect ratio ($a/b = 1$) and boundary conditions.

II.6 *Numerical Simulation (Finite Element Method)*

Numerical validation was conducted using Solidworks 2022 Simulation software with the following setup parameters:

A. *Element discretization (meshing)*

Given the small thickness-to-span ratio ($t/L < 0.01$), the model was discretized using second-order (parabolic) Shell Elements. A mesh convergence study was performed to ensure result accuracy in stress concentration areas at the bottom corners of the tank[35]. Figure 4 shows the model to be analyzed using Solidworks 2022 simulation software.

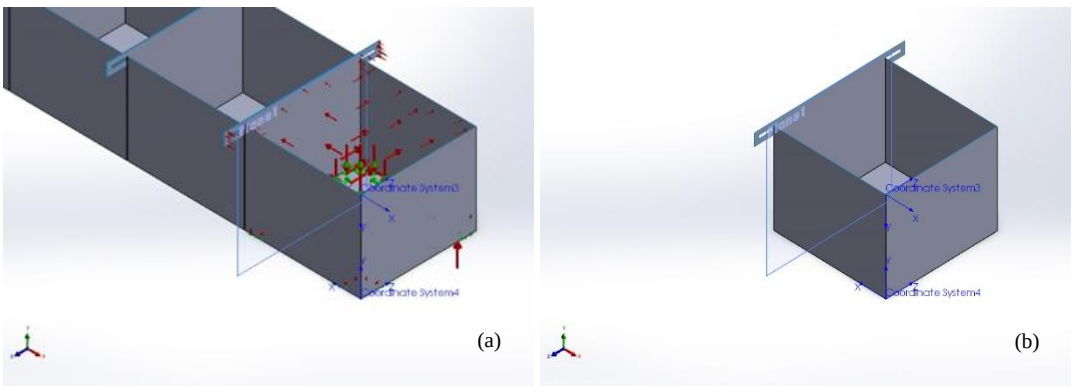

Figure 4. (a) Original Shell Element Model and (b) Analyzed Shell Element Model

B. *Loading and boundary conditions*

Fixtures: fixed geometry was applied to the panel base and vertical sides to represent the stiffness of the modular joints and the concrete floor. Loading: non-uniform pressure was applied to the inner wall surface with a gradient equation of $P = 19{,}620\ \text{Pa}$ at the tank bottom ($y = 0\ \text{mm}$) and $0\ \text{Pa}$ at the water surface ($y = 2000\ \text{mm}$)[36]. Figure 5 shows the fixed geometry boundary condition on the towing tank panel base and the loading applied to the towing tank wall in Solidworks 2022 software.

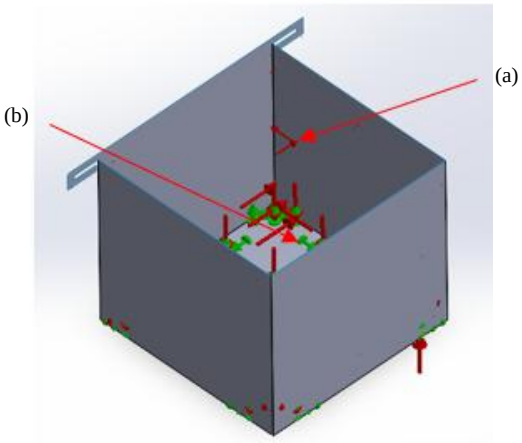

Figure 5. (a) Definition of Non-Uniform Hydrostatic Load on the Towing Tank Wall and (b) Application of Boundary Conditions (Fixed Support) on the Towing Tank Panel Base.

C. *Failure criterion*

Given the orthotropic nature of the GFRP material, the Von Mises failure criterion was not utilized[12]. Structural integrity evaluation was based on the Tsai-Hill criterion, which accounts for the interaction of normal and shear stresses in laminated composites:

$$\left(\frac{\sigma_1}{X}\right)^2 - \frac{\sigma_1\sigma_2}{X^2} + \left(\frac{\sigma_2}{Y}\right)^2 + \left(\frac{\tau_{12}}{S}\right)^2 < 1 \quad \text{.....(4)}$$

Where X and Y are the longitudinal and transverse tensile strengths of the material, respectively, and S is the shear strength[37]. The structure is declared safe if the failure index is < 1.

II.7 *Design Acceptance Criteria*

The final design validation requires satisfaction of two distinct limit states mandated by composite pressure vessel design standards and precision measurement facility operational requirements. The design is declared valid and optimal if it meets two limit states:

A. *Serviceability limit state (SLS)*

The maximum wall deflection (δ_{max}) must not exceed $L/200$ (10 mm) to ensure the accuracy of the towing carriage trajectory[38].

$$\delta_{max} \leq \frac{2000}{200} = 10\ \text{mm} \quad \text{.....(5)}$$

B. *Ultimate limit state (ULS)*

The minimum safety factor is 3.0 - 4.0, referring to the ASME RTP-1 standard for non-metallic pressure vessels, to compensate for environmental degradation factors (osmosis) and material fatigue[19][39].

$$SF = \frac{\sigma_{yield}}{\sigma_{working}} \geq 3.0 \quad \text{..... (6)}$$

Where:

σ_{yield} = yield strength of the GFRP material,

$\sigma_{working}$ = stress acting on the material.

This deflection limit ensures towing carriage rail alignment accuracy within ±5 mm tolerance for precise hydrodynamic measurements[29].

III. RESULT AND DISCUSSION

This chapter outlines the findings of the structural integrity analysis of the modular GFRP towing tank. The evaluation was conducted through a comparison between analytical predictions (as a baseline) and full-scale numerical simulation results (2×2 meters) to identify structural behaviors not predicted by simple manual calculations.

III.1 Analytical Prediction (Baseline Calculation)

Initial calculations were performed using Kirchhoff-Love Plate Theory (Roark's Formulation) on a single critical panel with dimensions of $2{,}000 \times 2{,}000$ mm. With a hydrostatic load input of $P_{max} = 19{,}620\ Pa$ and a wall thickness increased to $t = 19\ mm$ (26 layers), the theoretical structural response characteristics were obtained as presented in Table 2:

TABLE 2.
ANALYTICAL CALCULATION RESULTS (ROARK'S FORMULAS)

Parameter	Equation	Calculation Result	Allowable Limit	Status
Max Bending Stress (σ_{max})	$\sigma_{max} = \beta \cdot \frac{P_{max} \cdot b^2}{t^2}$	26.09 MPa	150 MPa	Safe
Max Deflection (y_{max})	$y_{max} = \alpha \cdot \frac{P_{max} \cdot b^4}{E \cdot t^3}$	5.95 mm	10 mm	Safe

Note: Coefficients $\beta = 0.12$ and $\alpha = 0.0013$ are used for a square plate with clamped edges.

III.2 Full Scale Numerical Analysis (FEM)

Finite Element Method simulations were performed on the full 2×2 meters towing tank module to capture the global structural behavior and more realistic

boundary conditions. The results of the numerical analysis are as follows:

A.Stress distribution

The von mises stress contours indicate that critical stresses are not uniformly distributed but are concentrated at the radius of the junction between the vertical wall and the base floor (fixed support). The recorded maximum nodal stress is 41 MPa, as illustrated in Figure 6.

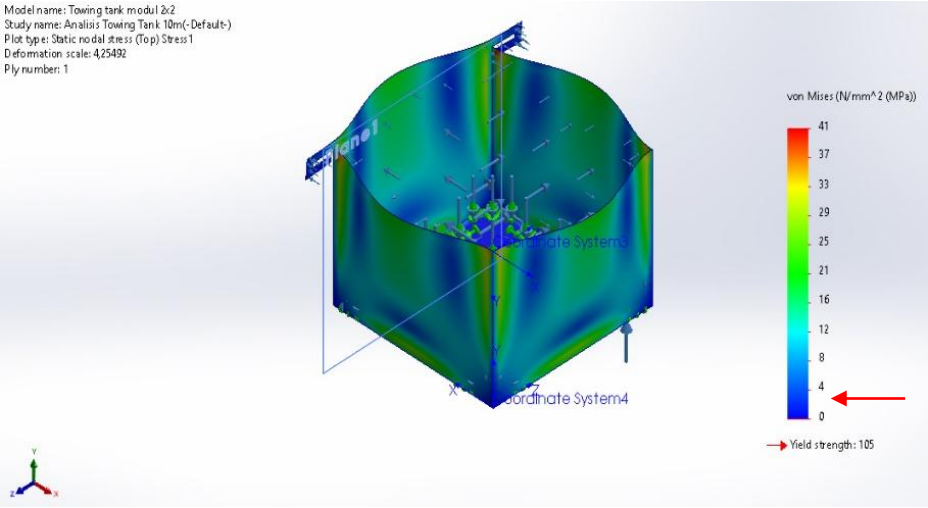

Figure 6. Von Mises Stress Contour on the 2×2 Meter Model

Despite the existence of stress concentrations, the value of 41 MPa is still far below the Ultimate Tensile Strength (UTS) of the GFRP material, which is 150 MPa. This results in a minimum Safety Factor of 3.65. This figure meets the ASME RTP-1 standard ($SF \geq 3.0 - 4.0$) for non-metallic vessels, meaning the tank wall is safe from the risk of material failure (rupture/cracking).

Unlike the stress analysis which showed positive results, the deformation analysis revealed a critical phenomenon in the structure's stiffness behavior. The simulation results recorded a maximum deflection (Resultant Displacement) of 62 mm, as shown in Figure 7. The deformation pattern indicates that the wall experiences extreme bulging at the top rim of the tank between the reinforcing flanges.

B. Displacement profile

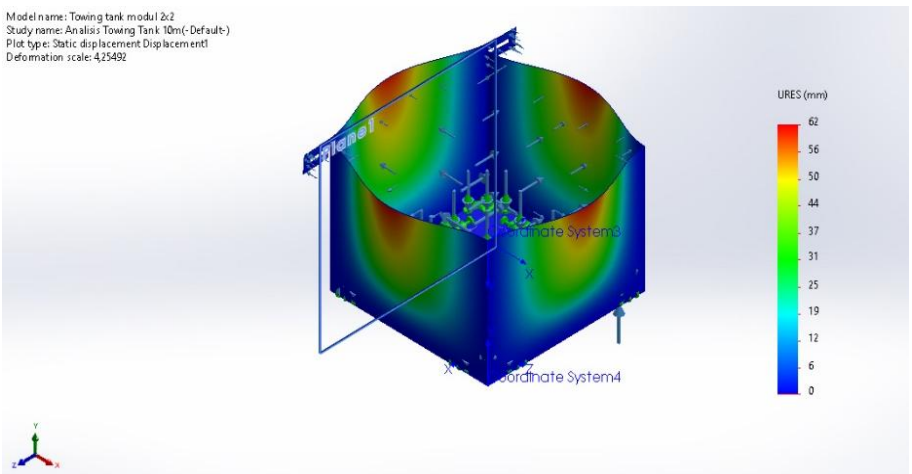

Figure 7. Side/Isometric View of Displacement Plot

This 62 mm deflection value exceeds the Serviceability Limit State (SLS) tolerance of $L/200$ (10 mm). This condition is operationally unacceptable as it causes significant geometric changes to the tank width when filled with water, potentially disrupting the path of the towing carriage rails.

III.3 Integrity Evaluation Based on Failure Criteria

The safety evaluation of the GFRP composite structure was conducted using criteria that account for the material's orthotropic properties.

A.....Analytical safety factor

Analytical safety factor calculated based on the ratio of the ultimate tensile strength ($X_{tensile}$) of the GFRP material (150 MPa) to the maximum bending stress analytical:

$$SF_{Analytical} = \frac{\sigma_{UTS}}{\sigma_{max\,(Roarks)}} = \frac{150\ \text{MPa}}{26.09\ \text{MPa}} \approx 5.75$$

With $SF = 5.75$, this design meets and exceeds the requirements of the ASME RTP-1 standard ($SF \geq 3.0$) and BKI Volume V for non-metallic structures [19][18].

A.....*Numerical safety factor*

The actual safety factor (SF_{actual}) is calculated based on the ratio of the ultimate tensile strength ($X_{tensile}$) of the GFRP material (150 MPa) to the maximum simulation working stress:

$$SF_{FEM} = \frac{\sigma_{UTS}}{\sigma_{max\,(FEM)}} = \frac{150\ \text{MPa}}{41\ \text{MPa}} \approx 3.65$$

With $SF = 3.65$, this design meets and exceeds the requirements of the ASME RTP-1 standard ($SF \geq 3.0$) and BKI Volume V for non-metallic structures [19][18]. Figure 8 presents the Safety Factor simulation results from Solidworks 2022 software with a value of 4.

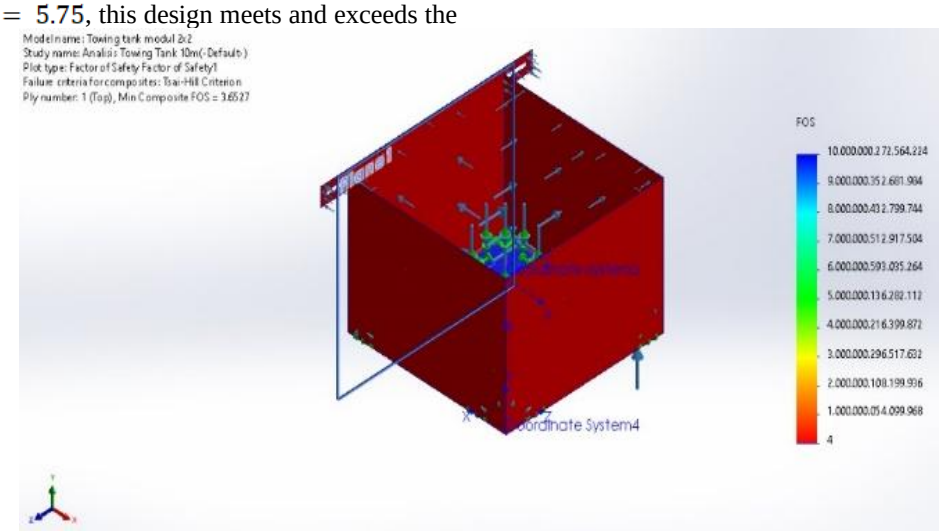

Figure 8. Safety Factor Simulation Result in Solidworks 2022 Software

III.4 Analytical and Numerical Disparity

The comparison between analytical and numerical methods reveals a significant disparity in data, particularly regarding the deflection parameter, as summarized in Table 3.

TABLE 3.
COMPARISON OF ANALYTICAL AND NUMERICAL RESULTS

Parameter	Analytical (Roark)	Numerical (FEM)	Deviation
Maximum Stress (MPa)	26.09	41.0	+57%
Maximum Deflection (mm)	5.95	62.0	+942%
Safety Factor	5.75	3.65	-36%
SLS Compliance	Pass (5.95 < 10)	Fail (62 > 10)	-

Note: Numerical values are simulation results under real boundary conditions (bolted flanges), whereas analytical results assume perfect rigid clamping.

Analysis of disparity causes: the extreme difference in deflection (5.95 mm vs 62 mm) is not caused by calculation errors, but rather by fundamental differences in boundary conditions representation. Analytical method (roark): assumes the plate is rigidly clamped on all four sides (top, bottom, left, right). This assumption is idealistic and considers that the tank's top rim is restrained by a rigid structure. Numerical method (FEM): represents the actual condition of an open-top tank, where the top side of the wall is a free edge with no lateral restraint.

These findings validate the hypothesis that for long rectangular tanks, the stiffness of the vertical plate alone (19 mm thickness) is insufficient to withstand hydrostatic pressure if the top section is free. The wall behaves like a wide cantilever beam, causing massive deflection at its free end[36]. In Figure 9 there is a comparison graph between the results of the analytical method and the results of the numerical method, depicted using a bar chart.

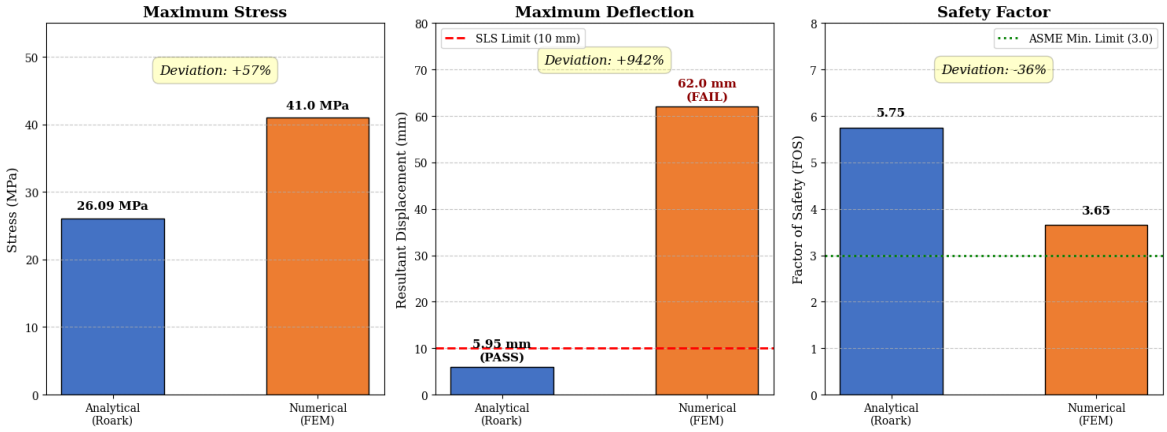

Figure 9. Bar Chart Comparison of Analytical Method (Roark's Theory) vs. Numerical Method (FEM)

The free top edge transforms the plate behavior from a doubly-fixed rectangular plate (analytical assumption) to a wide cantilever beam (actual condition). Without lateral restraint, hydrostatic pressure induces:

A. Primary bending: transverse deflection governed by plate stiffness ($D = Et^3/12(1-\nu^2)$).
B. Secondary rotation: top rim rotates outward, amplifying displacement through moment-curvature coupling.
C. Membrane tension development: at large deflections ($\frac{w}{t} = \frac{62}{19} = 3.26$), geometric nonlinearity introduces membrane stretching, partially stabilizing the structure but exceeding SLS limits[31].

Li et al. [35] reported similar phenomena in rectangular tanks with free edges, observing deflection amplification factors of $8-12\times$ compared to fully restrained cases. Our $10.4\times$ amplification ($62/5.95$) aligns with their findings for slender panels ($a/t = 105$). Naseri et al. [36] demonstrated that open-top cylindrical tanks experience rim deflections exceeding $L/100$ without stiffening rings validating the criticality of edge restraint in fluid containment structures.

III.5 Design Optimization Recommendations

The decision to increase the wall thickness to 19 mm with a 26-layer arrangement (13 WR + 13 CSM) proved to be a crucial optimization step. While the structure passes ultimate strength criteria, serviceability failure (62 mm > 10 mm deflection) renders the design operationally unacceptable. Based on the analysis above, it is concluded that the initial design failure mode is not a strength failure, but rather a stiffness failure[40]. The recommended engineering solution is to alter the "Free Edge" boundary condition to a "Simple Support" or "Elastic" condition by adding a horizontal Rim Stiffener[41]. The addition of an angle steel profile or composite beam (e.g., 50×50 mm L-profile) along the top rim of the tank will drastically increase the Moment of Inertia (I) of the top cross-section, which is predicted to reduce deflection from 62 mm back to the theoretical range (< 10 mm).

IV. CONCLUSION

This comprehensive structural analysis of a modular GFRP towing tank reveals critical insights into composite design for hydrodynamic testing facilities. Strength adequacy confirmed the 19 mm hybrid laminate (13 WR-800 + 13 CSM-450 layers) safely withstands 2 meter hydrostatic head with SF = 3.65, exceeding ASME RTP-1 and BKI marine standards. Serviceability failure identified free-edge effects produce 62 mm rim deflection 6.2× beyond L/200 acceptance criteria demonstrating that classical plate theory grossly underpredicts deformation in open-top configurations. Boundary condition criticality quantified analytical methods assuming fully clamped edges underestimate deflections by 942%, mandating full-scale FEM for realistic design validation. Design modification imperative horizontal rim stiffeners (50×50 mm L-profile minimum) are essential to restore global stiffness and achieve <10 mm deflection tolerance. Economic viability demonstrated, modular GFRP construction reduces capital costs by 65-70% compared to conventional concrete, enabling maritime research infrastructure deployment in resource-constrained institutions. This research establishes that successful composite tank design requires dual validation against ultimate strength and serviceability limits, with edge stiffness emerging as the governing design criterion for open-top modular configurations.

ACKNOWLEDGEMENTS

The authors gratefully acknowledge the Research and Community Service Institution (LPPM) Universitas Darma Persada for financial support of this research project.

REFERENCES

[1] R. Nepal, H. Phoumin, and A. Khatri, “Green technological development and deployment in the association of southeast Asian economies (ASEAN)—At crossroads or roundabout?,” *Sustain.*, vol. 13, no. 2, pp. 1–19, 2021, doi: https://doi.org/10.3390/su13020758.

[2] Ministry of National Development Planning/Bappenas, *Indonesia 2045: Sovereign, Advanced, Just, and Prosperous*. Jakarta, 2019.

[3] L. Huang, B. Pena, and G. Thomas, “Towards a full-scale CFD guideline for simulating a ship advancing in open water,” *Sh. Technol. Res. Schiffstechnik*, vol. 70, no. 3, pp. 222–238, 2023, doi: https://doi.org/10.1080/09377255.2023.2167537.

[4] Y. E. Lee *et al.*, "Development of a Modular Low-Cost Wave Tank for Educational and Small-Scale Experimental Applications : A Practical Approach," in *APS Proceedings*, 2025, pp. 202–207. doi: 10.5281/zenodo.16034141.

[5] G. Mai, Z. Xiong, H. Zhu, L. Zhou, H. Zhou, and L. Li, "Durability of GFRP bars embedded in seawater sea sand concrete in marine environments.," *Constr. Build. Mater.*, vol. 458, 2025, doi: https://doi.org/10.1016/j.conbuildmat.2024.139488.

[6] R. Li, X. Zheng, H. Wang, S. Xiong, K. Yan, and P. Li, "New analytic buckling solutions of rectangular thin plates with all edges free," *Int. J. Mech. Sci.*, vol. 144, pp. 67–73, 2018, doi: https://doi.org/10.1016/j.ijmecsci.2018.05.041.

[7] B. Rashid, A. Sadeq, M. Ebraheem, and A. R. Mohammed, "Mechanical properties of hybrid woven roving and chopped strand mat glass fabric reinforced polyester composites," *Mater. Res. Express*, vol. 6, no. 105208, 2019, doi: https://doi.org/10.1088/2053-1591/ab4085.

[8] John C. Daidola, "Modularity: Facilitator for Commercial Shipyards in Naval Shipbuilding," *J. Sh. Prod. Des.*, vol. 37, no. 02, pp. 97–108, 2021, doi: https://doi.org/10.5957/JSPD.11190059.

[9] A. Alhajahmad and C. Mittelstedt, "Thin-Walled Structures Minimum weight design of curvilinearly grid-stiffened variable-stiffness composite fuselage panels considering buckling and manufacturing constraints," *Thin-Walled Struct.*, vol. 161, no. December 2020, p. 107526, 2021, doi: 10.1016/j.tws.2021.107526.

[10] P. Różyło, P. Wysmulski, And K. Falkowicz, "FEM And Experimental Analysis of Thin-Walled Composite Element performance of e-glass reinforced polyester resins (isophthalic and orthophthalic) laminate composites used in marine applications," *J. Mater. Des. Appl.*, vol. 238, no. 4, 2024, doi: https://doi.org/10.1177/14644207231194437.

[18] Indonesian Classification Bureau (BKI), "Rules for the Classification and Construction of Seagoing Ships, Vol I: Rules for Material.," 2022, *BKI, Jakarta*.

[19] ASME, "ASME RTP-1-2023: Reinforced Thermoset Plastic Corrosion-Resistant Equipment. New York: American Society of Mechanical Engineers," 2023.

[20] R. Aranha *et al.*, "Effect of Water Absorption and Stacking Sequences on the Tensile Properties and Damage Mechanisms of Hybrid Polyester / Glass / Jute Composites," *Polymers (Basel).*, vol. 16, no. 925, 2024, doi: https://doi.org/10.3390/ polym16070925.

[21] S. A. Rahmawaty, A. Wahyu, Y. Putra, and A. D. Laksono, "Tensile and Bending Strength Analysis of Glass Fiber-Polyester Composites with Variations in Fiber Volume Fraction," *J. Mech. Eng. – ITI*, vol. 5, no. 3, pp. 146–155, 2021.

[22] F. Rubino, A. Nisticò, F. Tucci, and P. Carlone, "Marine Application of Fiber Reinforced Composites : A Review," *Mar. Sci. Eng.*, vol. 8, no. 26, 2020, doi: doi:10.3390/jmse8010026.

[23] MatWeb: Material Property Data, "Overview of materials for Glass Reinforced Polyester (GRP)," 2024.

[24] K. K. Chawla, *Composite Materials: Science and Engineering*, Third Edit. Springer Science & Business Media., 2012.

[25] Robert M. Jones, *Mechanics Of Composite Materials*, 2nd Editio. Boca Raton: CRC Press, 2018. doi: https://doi.org/10.1201/9781498711067.

[26] Autar K. Kaw, *Mechanics of Composite Materials*, 2nd Editio. Boca Raton: CRC Press, 2005.

[27] J. N. Reddy, *Mechanics of laminated composite plates and shells: theory and analysis. CRC press*. USA: CRC Press, 2003.

[28] P.K. Mallick, *Fiber-Reinforced Composites Materials, Manufacturing, and Design*, Third Edit. Boca Raton: CRC Press, 2007. doi: https://doi.org/10.1201/9781420005981.

[29] M. Bazli *et al.*, "Durability of glass-fibre-reinforced polymer composites under seawater and sea-sand concrete coupled with harsh outdoor environments," 2020, doi: 10.1177/1369433220947897.

[30] US Department of Defense, *Composite Materials Handbook Under Compression*," *Int. J. Appl. Mech. Eng.*, vol. 22, no. 2, pp. 393–402, 2017, doi: 10.1515/ijame-2017-0023.

[11] I. Mititelu *et al.*, "Multi-Criteria Evaluation of the Failure of CFRP Laminates for Frames in the Automotive Industry," *Polymers (Basel).*, vol. 14, no. 21, p. 4507, 2022, doi: https://doi.org/10.3390/polym14214507.

[12] S. D. Müzel, E. P. Bonhin, N. Miranda, and E. S. Guidi, "Application of the Finite Element Method in the Analysis of Composite Materials : A Review," *Polymers (Basel).*, vol. 12, no. 818, 2020, doi: https://doi.org/10.3390/polym12040818.

[13] P. Davies, "Environmental degradation of composites for marine structures : new materials and new applications," *Philos. Trans. R. Soc. A Math. Phys. Eng. Sci.*, vol. 374, no. 2071, 2016, doi: https://doi.org/10.1098/rsta.2015.0272.

[14] L. Prabhu, V. Krishnaraj, S. Sathish, and V. Sathyamoorthy, "Experimental and Finite Element Analysis of GFRP Composite Laminates with Combined Bolted and Bonded Joints," *Indian J. Sci. Technol.*, vol. 10, no. 14, 2017, doi: 10.17485/ijst/2017/v10i14/104606.

[15] T. Garbowski, P. Borecki, J. Rutkowski, And Anna Szymczak-Graczyk, "Optimal Design Of Rectangular Tank Walls With Ribs Using Numerical Models And Global Optimization," *Civ. Environ. Eng. Reports*, Vol. 34, No. 4, Pp. 293–306, 2024, Doi: 10.59440/Ceer/195601.

[16] B. Liu, Y. Garbatov, L. Zhu, and C. G. Soares, "Numerical assessment of the structural crashworthiness of corroded ship hulls in stranding," *Ocean Eng.*, vol. 170, no. October, pp. 276–285, 2018, doi: 10.1016/j.oceaneng.2018.10.034.

[17] S. Ojha, H. Bisaria, S. Mohanty, and K. Kanny, "Mechanical

(MIL-HDBK-17-2F). 2002.

[31] A. C. Ugural, *Plates and Shells: Theory and Analysis*, 4th Editio. Boca Raton: CRC Press, 2017. doi: https://doi.org/10.1201/9781315104621.

[32] L. Shi, J. Shuai, X. Wang, and K. Xu, "Experimental and numerical investigation of stress in a large-scale steel tank with a floating roof," *Thin Walled Struct.*, vol. 117, pp. 25–34, 2017, doi: 10.1016/j.tws.2017.03.037.

[33] A. M. Young, W. C., Budynas, R. G., & Sadegh, *Roark's formulas for stress and strain*, Vol.7. New York: Mc Graw Hill, 2002.

[34] E. J. Barbero, *Introduction to composite materials design*, Second. CRC Press, 2010.

[35] K. Wang and L. Li, "Structural analysis and optimal design of a spherical thin-walled stainless steel water tank without reinforced tie ribs," *J. VIBROENGINEERING*, vol. 26, no. 4, pp. 983–1000, 2024, doi: 10.21595/jve.2024.23812.

[36] H. Naseri, T. Zirakian, and H. Showkati, "Stability response assessment of steel thin-walled open-top tanks subjected to local support edge settlement," *World J. Eng.*, vol. 22, no. 1, pp. 29–29, 2023, doi: 10.1108/WJE-06-2023-0165.

[37] M. Lezgy-Nazargah, "Assessment of refined high-order global–local theory for progressive failure analysis of laminated composite beams," *Acta Mech.*, vol. 228, pp. 1923–1940, 2017, doi: 10.1007/s00707-017-1807-6.

[38] A. Alhayek *et al.*, "Flexural Creep Behaviour of Pultruded GFRP Composites Cross-Arm : A Comparative Study on the Effects of Stacking Sequence," *Polymers (Basel).*, vol. 14, no. 1330, 2022, doi: https://doi.org/10.3390/ polym14071330.

[39] G. Vizentin and G. Vukelic, "Degradation and Damage of Composite Materials in Marine Environment," *Mater. Sci. (MEDŽIAGOTYRA).*, vol. 26, no. 3, 2020, doi: http://dx.doi.org/10.5755/j01.ms.26.3.22950 Received.

[40] S. M. Jensen, B. L. V Bak, J. J. Bender, L. Carreras, and E. Lindgaard, "Transient delamination growth in GFRP laminates with fibre bridging under variable amplitude loading in G-control," *Compos. Part B*, vol. 225, no. 109296, 2021, doi: 10.1016/j.compositesb.2021.109296.

[41] Richard G. Budynas et.al, *Shigley's Mechanical Engineering Design*. Mc Graw Hill, 2011.